PRECONDITIONING FOR VECTOR-VALUED CAHN–HILLIARD EQUATIONS

JESSICA BOSCH

Numerical Linear Algebra for Dynamical Systems, Max Planck Institute for Dynamics of Complex Technical Systems, Sandtorstr. 1, 39106 Magdeburg, Germany

Abstract. The solution of vector-valued Cahn–Hilliard systems is of interest in many applications. We discuss strategies for the handling of smooth and nonsmooth potentials as well as for different types of constant mobilities. For the latter, the necessary bound constraints are incorporated via the Moreau–Yosida regularization technique. We develop effective preconditioners for the efficient solution of the linear systems in saddle point form. Numerical results illustrate the efficiency of our approach. In particular, we numerically show mesh and phase independence of the developed preconditioner in the smooth case. The results in the nonsmooth case are also satisfying and the preconditioned version always outperforms the unpreconditioned one.

1. Introduction

The Cahn–Hilliard equation is a partial differential equation of fourth order, which is used in materials science [18], image processing [13] or chemistry [33]. It was originally introduced to model phase separation in binary alloys [23, 10] that occurs when the temperature of a homogeneous mixture is rapidly quenched below a critical temperature. In practice, often more than two phases occur, see e.g. [28, 17, 15, 14, 5, 26, 20], and the phase field model has been extended to deal with multi-component systems. A vector-valued order parameter $\mathbf{u} = (u_1, \dots, u_N)^T : \Omega \times (0, T) \to \mathbb{R}^N$ is introduced, where $\Omega \subset \mathbb{R}^d$ ($d = 1, 2, 3$) is a bounded domain, $T > 0$ is an arbitrary but fixed time and N is the number of phases. Each u_i describes the fraction of one phase, i.e. if $u_i = 0$ then the phase i is absent in that region and if $u_i = 1$ only phase i is present in that region. Hence,

$$\sum_{i=1}^{N} u_i = 1 \tag{1}$$

and $u_i \geq 0$ is required, so that admissible states belong to the Gibbs simplex

$$\mathcal{G}^N := \left\{ \mathbf{v} \in \mathbb{R}^N \;\middle|\; \sum_{i=1}^{N} v_i = 1,\ v_i \geq 0 \text{ for } i = 1, \dots, N \right\}.$$

We study a diffuse phase transition, i.e. the region between the phases has a certain width b, the so-called interface (phase field model). There is also the limit case $b \downarrow 0$ which gives the sharp interface model [19, 18]. The motion of the interfaces separating N bulk regions is modeled with the Ginzburg–Landau energy

$$\mathcal{E}(\mathbf{u}) = \int_\Omega \frac{\varepsilon^2}{2} \sum_{i=1}^{N} |\nabla u_i|^2 + \psi(\mathbf{u}) \, \mathrm{d}\mathbf{x},$$

where $\varepsilon > 0$ is the gradient energy coefficient. The potential function $\psi : \mathbb{R}^N \to \mathbb{R}_0^+ \cup \{\infty\}$ gives rise to phase separation. It can be modeled by a smooth free energy, e.g. using multi-well potentials

E-mail address: bosch@mpi-magdeburg.mpg.de.

[31] such as

$$\psi(\mathbf{u}) := \frac{1}{4}\sum_{i=1}^{N} u_i^2(1-u_i)^2, \tag{2}$$

or by a nonsmooth multi obstacle potential [3]

$$\psi(\mathbf{u}) := \begin{cases} \psi_0(\mathbf{u}) = -\frac{1}{2}\mathbf{u}\cdot A\mathbf{u} & \mathbf{u}\in\mathcal{G}^N, \\ \infty & \text{otherwise}, \end{cases} \tag{3}$$

where the symmetric matrix $A \in \mathbb{R}^{N\times N}$ contains constant interaction parameters A_{ij}. From physical considerations A must have at least one positive eigenvalue. A typical choice is $A = I - \mathbf{1}\mathbf{1}^T$ with $\mathbf{1} = (1,\dots,1)^T$, which means that the interaction between all different components is equal and no self-interaction occurs. Other possible potentials are logarithmic ones, see e.g. [2]. This work deals with the two types of potential (2) and (3). The smooth potential (2) is used for shallow temperature quenches. It has the disadvantage that physically non-admissible values $u_i < 0$ or $u_i > 1$ can be attained during the evolution, see section 5. The consideration of the deep quench limit, i.e. a very rapid cooling of the mixture, leads to the multi obstacle potential (3). It omits the disadvantage of (2) but leads to a system of variational inequalities. Motivated by the work of Hintermüller, Hinze and Tber [24] as well as our previous studies [8, 7], all of them considering scalar, nonsmooth Cahn–Hilliard systems, we incorporate the bound constraints via the Moreau–Yosida regularization technique and solve the resulting subproblems by a semismooth Newton (SSN) method.

As we show in the course of this paper the solution of a linear system $\mathcal{K}x = b$ with a real nonsymmetric matrix $\mathcal{K}$ is at the heart of this method. The sparse linear systems are usually of very large dimension and in combination with three-dimensional experiments the application of direct solvers such as UMFPACK [12] becomes infeasible. As a result iterative methods have to be employed (see e.g. [21] for an introduction to this field). We propose the use of a Krylov subspace solver. The convergence behavior of the iterative scheme typically depends on the conditioning of the problem and the clustering of the eigenvalues. These properties can be enhanced using preconditioning techniques $\mathcal{P}^{-1}\mathcal{K}x = \mathcal{P}^{-1}b$, where $\mathcal{P}$ is an invertible matrix that is easy to invert and resembles $\mathcal{K}$. In this paper, we provide efficient preconditioners $\mathcal{P}$ for the solution of Cahn–Hilliard variational (in-)equalities using an effective Schur complement approximation and (algebraic) multigrid developed for elliptic systems [30].

The paper is organized as follows. In section 2 we derive the vector-valued Cahn–Hilliard equations. These are discretized in time and space in section 3. In section 4, we analyze the linear systems and propose preconditioning strategies for the saddle point problems. Section 5 illustrates the efficiency of our approach and section 6 summarizes our findings.

2. Derivation

The evolution of $\mathbf{u}$ is governed by the H^{-1}-gradient of the Ginzburg–Landau energy under the constraint (1), which has to hold everywhere at any time. Using the smooth potential (2), the vector-valued Cahn–Hilliard equations reads

$$\frac{\partial u_i}{\partial t} = (L\Delta\mathbf{w})_i, \tag{4}$$

$$w_i = f(u_i) + \beta(\mathbf{u}) - \varepsilon^2\Delta u_i, \tag{5}$$

$$\nabla u_i\cdot\mathbf{n} = (L\nabla\mathbf{w})_i\cdot\mathbf{n} = 0 \quad \text{on } \partial\Omega, \tag{6}$$

for $i = 1,\dots,N$, where $L = (L_{ij})_{i,j=1,\dots,N} \in \mathbb{R}^{N\times N}$ is the mobility, $\frac{\partial\psi}{\partial\mathbf{u}} = \left(\frac{\partial\psi}{\partial u_1},\dots,\frac{\partial\psi}{\partial u_N}\right)^T = \mathbf{f}(\mathbf{u}) = (f(u_1),\dots,f(u_N))^T$, in which $f(u_i) = u_i^3 - \frac{3}{2}u_i^2 + \frac{1}{2}u_i$, and $\beta(\mathbf{u}) = -\frac{1}{N}\sum_{i=1}^{N} f(u_i)$. In the process, the chemical potentials $\mathbf{w} = (w_1,\dots,w_N)^T$ result from the variational derivative of the energy $\mathcal{E}$. In doing so, admissible directions $\mathbf{d} = (d_1,\dots,d_N)^T$ have to fulfill $\sum_{i=1}^{N} d_i = 0$ in order to ensure (1).

This explains the presence of the term $\beta(\mathbf{u})$. Equation (6) contains the natural zero Neumann boundary condition $\nabla u_i \cdot \mathbf{n} = 0$ on $\partial\Omega$ as well as the mass conserving boundary condition $(L\nabla\mathbf{w})_i = 0$ on $\partial\Omega$, $i = 1,\dots,N$. Since using the latter in (4) yields together with Gauss's theorem $\frac{\mathrm{d}}{\mathrm{d}t}\int_\Omega u_i \,\mathrm{d}\mathbf{x} = 0$, i.e. the total mass of each phase is conserved.

The coefficients L_{ij} may depend on $\mathbf{u}$ (see [14]) but this work deals with constant L_{ij}. It is assumed that L is symmetric and either $L\mathbf{1} = \mathbf{0}$ or $L = I$ as summing (4) over $i = 1,\dots,N$ leads to

$$\frac{\partial}{\partial t}\sum_{i=1}^N u_i = \sum_{i=1}^N \frac{\partial u_i}{\partial t} \overset{(4)}{=} \sum_{i=1}^N \nabla\cdot(L\nabla\mathbf{w})_i = \nabla\cdot\sum_{i,j=1}^N L_{ij}\nabla w_j = \nabla\cdot\sum_{j=1}^N \nabla w_j \sum_{i=1}^N L_{ij} = 0. \tag{7}$$

Hence, if the initial data $\mathbf{u}(\mathbf{x},0)$ fulfills (1) for all $\mathbf{x}\in\Omega$, then (1) holds $\forall t > 0$. It is further assumed that L is positive semidefinite as differentiating the energy $\mathcal{E}$ gives

$$\frac{\mathrm{d}}{\mathrm{d}t}\mathcal{E}(\mathbf{u}) = -\int_\Omega \sum_{i=1}^N \nabla w_i \cdot (L\nabla\mathbf{w})_i \,\mathrm{d}\mathbf{x} \le 0,$$

where we used (4)–(6) and Green's first identity. Therefore, the total energy is non-increasing.

If we now use the nonsmooth multi obstacle potential (3), the gradient of $\mathcal{E}$ employs subdifferentials which results in the following vector-valued Cahn–Hilliard variational inequalities

$$\left\langle \frac{\partial u_i}{\partial t}, v\right\rangle + ((L\nabla\mathbf{w})_i, \nabla v) = 0 \quad \forall v\in H^1(\Omega), \tag{8}$$

$$\varepsilon^2(\nabla u_i, \nabla(v_i - u_i)) - \left(w_i + (A\mathbf{u})_i - \frac{1}{N}\sum_{j=1}^N (A\mathbf{u})_j, v_i - u_i\right) \ge 0 \quad \forall \mathbf{v}\in\mathcal{G}^N\cap H^1(\Omega)^N, \tag{9}$$

$$\mathbf{u}\in\mathcal{G}^N\cap H^1(\Omega)^N \text{ a.e. in } \Omega, \tag{10}$$

for $i = 1,\dots,N$. Here $(\cdot,\cdot)$ and $\langle\cdot,\cdot\rangle$ stand for the $L^2(\Omega)$-inner product and the duality pairing of $H^1(\Omega)$ and $H^1(\Omega)^*$, respectively. We now want to discretize the problems (4)–(6) (in weak formulation) and (8)–(9) in time and space. Moreover, we shortly present a strategy which handles the variational inequalities.

3. Discretization

Concerning the time, fully implicit discretizations are the most accurate, see e.g. [4, 9, 8]. Let $\tau > 0$ denote the time step size and $n\in\mathbb{N}$ the time step. We use the backward Euler discretization for the time derivative $\partial_t u_i$, $i = 1,\dots,N$, and treat all the other terms implicitly. Then, for every time step we have to solve the time-discrete system

$$\left(u_i - u_i^{(n-1)}, v\right) + \tau\left((L\nabla\mathbf{w})_i, \nabla v\right) = 0 \quad \forall v\in H^1(\Omega), \tag{11}$$

$$\varepsilon^2(\nabla u_i, \nabla(v_i - u_i)) - \left(w_i + (A\mathbf{u})_i - \frac{1}{N}\sum_{j=1}^N (A\mathbf{u})_j, v_i - u_i\right) \ge 0 \quad \forall \mathbf{v}\in\mathcal{G}^N\cap H^1(\Omega)^N, \tag{12}$$

$$\mathbf{u}\in\mathcal{G}^N\cap H^1(\Omega)^N \text{ a.e. in } \Omega, \tag{13}$$

where we write $\mathbf{u}^{(n)} = \mathbf{u}$ and $\mathbf{w}^{(n)} = \mathbf{w}$. Analogously, we obtain the time-discrete system for the smooth Cahn–Hilliard equations (4)–(6).

As motivated in [24, 8, 7], we handle the pointwise constraints in (13) with a Moreau–Yosida regularization technique. Instead of the energy functional $\mathcal{E}$ we consider

$$\mathcal{E}_\nu(\mathbf{u}_\nu) = \int_\Omega \frac{\varepsilon^2}{2}\sum_{i=1}^N |\nabla u_{\nu,i}|^2 + \psi_0(\mathbf{u}_\nu) + \frac{1}{2\nu}\sum_{i=1}^N |\min(0, u_{\nu,i})|^2 \,\mathrm{d}\mathbf{x},$$

such that we obtain

$$\left(u_{v,i} - u_{v,i}^{(n-1)}, v\right) + \tau\left((L\nabla \mathbf{w}_v)_i, \nabla v\right) = 0 \quad \forall v \in H^1(\Omega), \tag{14}$$

$$(w_{v,i}, v) - \varepsilon^2(\nabla u_{v,i}, \nabla v) + ((A\mathbf{u}_v)_i, v) - \frac{1}{\nu}(\min(0, u_{v,i}), v) + \frac{1}{N}\sum_{j=1}^{N}\left[\frac{1}{\nu}(\min(0, u_{v,j}), v) - ((A\mathbf{u})_j, v)\right] = 0 \quad \forall v \in H^1(\Omega), \tag{15}$$

for $i = 1, \dots, N$, where $0 < \nu \ll 1$ denotes the penalty parameter. Now, in order to get the linear systems of equation, we apply the function space-based algorithm motivated in [24, 8, 7]. For a specified sequence $\nu \to 0$ we solve the optimality system (14)–(15), which can be written as $\mathbf{F}_\nu(\mathbf{u}_\nu, \mathbf{w}_\nu) = \mathbf{0}$, for every ν by an SSN algorithm, see also [25]. The smooth nonlinear time-discrete Cahn–Hilliard equations for (4)–(6) are solved by the standard Newton method.

Next, the time-discrete systems are discretized in space by finite elements. Let $\{\mathcal{R}_h\}_{h>0}$ be a triangulation of Ω into disjoint open rectangular elements with maximal element size h and J_h be the set of nodes of $\mathcal{R}_h$. The use of rectangles is motivated by performing the implementation with deal.II [1]. We approximate the infinite-dimensional space $H^1(\Omega)$ by the finite-dimensional space

$$S_h := \left\{\phi \in C^0(\bar{\Omega})\colon \phi|_R \in Q_1(R) \ \ \forall R \in \mathcal{R}_h\right\} \subset H^1(\Omega)$$

of continuous, piecewise multilinear functions. We denote the standard nodal basis functions of S_h by χ_j for all $j \in J_h$. Then, a function $u_h \in S_h$ is given by $u_h = \sum_{j\in J_h} u_{h,j}\chi_j$ and the vector of coefficients is now denoted by $\mathbf{u}$. Moreover, we use the lumped mass scalar product $(f,g)_h = \int_\Omega I_h(fg)$ instead of (f,g). The interpolation operator $I_h\colon C^0(\bar{\Omega}) \to S_h$ is defined by $(I_h f)(p_j) = f(p_j)$ for all nodes $j \in J_h$ where p_j denotes the coordinates corresponding to the node j. In matrix form, the fully discrete linear systems read

$$\begin{bmatrix} I \otimes M & -\mathcal{B} \\ \tau L \otimes K & I \otimes M \end{bmatrix}\begin{bmatrix} \mathbf{w}^{(k)} \\ \mathbf{u}^{(k)} \end{bmatrix} = \begin{bmatrix} \mathbf{b}_1 \\ \mathbf{b}_2 \end{bmatrix}, \tag{16}$$

where k denotes the Newton step and the superscript $^{(\text{old})}$ marks the solution from the previous time step. Further, $K := ((\nabla\chi_i, \nabla\chi_j))_{i,j=1,\dots,N} \in \mathbb{R}^{m\times m}$ is the stiffness matrix, $M := ((\chi_i, \chi_j))_{i,j=1,\dots,N} \in \mathbb{R}^{m\times m}$ is the lumped mass matrix and $I \in \mathbb{R}^{N\times N}$ is the identity. M is a symmetric positive definite diagonal matrix and K is symmetric and positive semidefinite. For $N = 3$, the block $\mathcal{B}$ is given as

$$\mathcal{B} = \begin{bmatrix} B_{11} & B_2 & B_3 \\ B_1 & B_{22} & B_3 \\ B_1 & B_2 & B_{33} \end{bmatrix},$$

where for $i = 1, \dots, N$

$$(a) \quad \begin{aligned} B_{ii} &= \varepsilon^2 K + \left(1 - \frac{1}{N}\right) F_i M F_i, \\ B_i &= -\frac{1}{N} F_i M F_i, \\ F_i &= \operatorname{diag}\left(3(u_i^{(k)})^2 - 3u_i^{(k)} + \frac{1}{2}\right), \end{aligned} \qquad (b) \quad \begin{aligned} B_{ii} &= \varepsilon^2 K + \left(1 - \frac{1}{N}\right)\left(\frac{1}{\nu} G_i M G_i - M\right), \\ B_i &= -\frac{1}{N}\left(\frac{1}{\nu} G_i M G_i - M\right), \\ G_i &= \operatorname{diag}\begin{pmatrix} 1 & u_i^{(k)}(p_j) < 0, \\ 0 & \text{otherwise}, \end{pmatrix} \end{aligned}$$

in the smooth system (a) and in the nonsmooth system (b). This work uses $A = (I - \mathbf{1}\mathbf{1}^T)$ (mentioned in the introduction) as well as $L = I$ and $L = I - \frac{1}{N}\mathbf{1}\mathbf{1}^T$ (a special case of the mobility matrix used e.g. in [14]). The system matrix in (16) is denoted by $\mathcal{K}$ for the remainder of the paper.

4. Preconditioning

In both cases, smooth and nonsmooth, a linear nonsymmetric system in saddle point form is at the heart of the computation. We propose the block-triangular preconditioner

$$\mathcal{P} = \begin{bmatrix} I \otimes M & 0 \\ \tau L \otimes K & -\hat{\mathcal{S}} \end{bmatrix}, \tag{17}$$

motivated by [16, 29], where $\hat{\mathcal{S}}$ is an approximation of the Schur complement $\mathcal{S} = I \otimes M + \tau(L \otimes K)(I \otimes M)^{-1}\mathcal{B}$. The preconditioned matrix $\mathcal{P}^{-1}\mathcal{K}$ has $N \cdot m$ eigenvalues at 1 and the remaining ones are characterized as the eigenvalues of the matrix $\hat{\mathcal{S}}^{-1}\mathcal{S}$, which for $\hat{\mathcal{S}}$ being a good approximation only has a small number of different eigenvalues. Inverting the $(1,1)$-block of $\mathcal{P}$ is cheap since M is a nonsingular diagonal matrix[1]. The remaining task is now to create a Schur complement approximation $\hat{\mathcal{S}}$ that is easy to invert and resembles $\mathcal{S}$. In doing so, the nondiagonal, nonsymmetric block matrix $\mathcal{B}$ poses the most difficult part. Concerning the nondiagonal block $L \otimes K$ with $L = I - \frac{1}{N}\mathbf{1}\mathbf{1}^T$ we can apply an effective Fast Fourier Transform (FFT) based preconditioner as L is a circulant matrix, see section 4.1. In the following we discuss the choice of $\hat{\mathcal{S}}$ first for the smooth and second for the nonsmooth case.

4.1. **Schur complement preconditioner in the smooth case.** As we know, the order parameter u_i approximately fulfills $0 \lesssim u_i \lesssim 1$ for $i = 1, \dots, N$. Therefore, we can estimate $-2.5 \lesssim F_i \lesssim 3.5$ for $i = 1, \dots, N$. Together with the estimated order of entries $O(M) = h^2$ for the mass matrix we propose the following approximation of $\mathcal{B}$

$$\hat{\mathcal{B}} = I \otimes \left(\varepsilon^2 K + \left(1 - \frac{1}{N}\right) M\right),$$

and thus the Schur complement preconditioner

$$\begin{aligned} \hat{\mathcal{S}} = \hat{\mathcal{S}}_1 (I \otimes M)^{-1} \hat{\mathcal{S}}_2 &= \left(\frac{N}{N-1}(I \otimes M) + \tau(L \otimes K)\right)(I \otimes M)^{-1}\hat{\mathcal{B}} \\ &= I \otimes M + \tau(L \otimes K)(I \otimes M)^{-1}\hat{\mathcal{B}} + \frac{\varepsilon^2 N}{N-1}(I \otimes K). \end{aligned}$$

Let us first discuss the case $L = I$. Then, both $\hat{\mathcal{S}}_1$ and $\hat{\mathcal{S}}_2$ are block-diagonal and for the computation of $\hat{\mathcal{S}}^{-1}$ we approximate the inverse diagonal blocks of $\hat{\mathcal{S}}_1$ and $\hat{\mathcal{S}}_2$ with an algebraic multigrid (AMG) preconditioner. These diagonal blocks are symmetric positive definite and independent of the individual phases. Therefore, we do not need N different preconditioners concerning the block $\mathcal{B}$ but one, and additionally we do not have to recompute them at every step of the Newton method.

If $L = I - \frac{1}{N}\mathbf{1}\mathbf{1}^T$, then L is a circulant matrix and we apply an FFT based preconditioner which is introduced by Stoll in [32]. This circulant approach is based on the fact that the matrix L can be diagonalized using the Fourier matrix F, i.e.

$$L = F \operatorname{diag}(\lambda_1, \dots, \lambda_N) F^H,$$

see [11]. If we apply the FFT to the system $\hat{\mathcal{S}}_1 y = g$ we get an equivalent system with a block-diagonal matrix

$$(F^H \otimes I)\hat{\mathcal{S}}_1 (F \otimes I) = \frac{N}{N-1}(I \otimes M) + \tau \operatorname{diag}(\lambda_1, \dots, \lambda_N) \otimes K. \tag{18}$$

The eigenvalues of L are $\lambda_1 = 0$ and $\lambda_2 = \dots = \lambda_N = 1$. As the application of the Fourier transform will in general result in complex valued systems, we formulate the blocks in (18) to 2×2 real valued block systems. In detail, we have to solve two types of systems

[1] For consistent mass matrices the Chebyshev semi-iteration provides a powerful preconditioner.

$$\begin{bmatrix} \frac{N}{N-1}M & 0 \\ 0 & \frac{N}{N-1}M \end{bmatrix}\begin{bmatrix} \tilde{y}_r \\ \tilde{y}_c \end{bmatrix} = \begin{bmatrix} \tilde{g}_r \\ \tilde{g}_c \end{bmatrix}, \quad \begin{bmatrix} \frac{N}{N-1}M + \tau K & 0 \\ 0 & \frac{N}{N-1}M + \tau K \end{bmatrix}\begin{bmatrix} \tilde{y}_r \\ \tilde{y}_c \end{bmatrix} = \begin{bmatrix} \tilde{g}_r \\ \tilde{g}_c \end{bmatrix}.$$

The first of the above systems arises for the diagonal block with $\lambda_1 = 0$ and the second one for all the remaining eigenvalues λ_j. As in [32], we solve these real valued systems with a fixed number of steps of an inexact Uzawa-type method

$$\tilde{y}^{(l+1)} = \tilde{y}^{(l)} + \omega \mathcal{P}_1^{-1}\tilde{r}^{(l)},$$

where $r^{(l)}$ denotes the residual and ω is the relaxation parameter. $\mathcal{P}_1$ is a block-diagonal preconditioner whose inverse is done by inverting the blocks $\frac{N}{N-1}M$ or by using AMG approximations of the blocks $\frac{N}{N-1}M + \tau K$. Again, this preconditioner is independent of the individual phases. Section 5 shows the efficiency of the proposed preconditioning strategy for both cases of L. In particular, we numerically illustrate the independence of $\hat{\mathcal{S}}$ with respect to the parameters h and N.

4.2. **Schur complement preconditioner in the nonsmooth case.** Here, an approximation of the matrix $\mathcal{B}$ in block-diagonal form (as done in the smooth case) seems not to be of good quality. The blocks B_i contain the parameter $\frac{1}{\nu}$, where $\nu \to 0$, and thus have a large order and should not be neglected. The proposed strategy concerning the block $\mathcal{B}$ is the use of a block Jacobi method. Looking at the definition of the diagonal blocks B_{ii} of $\mathcal{B}$ we see that they are indefinite, which typically causes problems. Therefore, we modify the preconditioner $\hat{\mathcal{S}}$ from the previous section to

$$\begin{aligned}\hat{\mathcal{S}} &= \hat{\mathcal{S}}_1(I \otimes M)^{-1}\hat{\mathcal{S}}_2 \\ &= \left(\frac{N}{N-1}(I \otimes M) + \sqrt{\tau}(L \otimes K)\right)(I \otimes M)^{-1}\left(\frac{N-1}{N}(I \otimes M) + \sqrt{\tau}\mathcal{B}\right) \\ &= I \otimes M + \tau(L \otimes K)(I \otimes M)^{-1}\mathcal{B} + \frac{\sqrt{\tau}\,N}{N-1}\mathcal{B} + \sqrt{\tau}\,\frac{N-1}{N}(L \otimes K).\end{aligned}$$

The approximation $\hat{\mathcal{S}}_1$ is already discussed in the previous section. The block $\hat{\mathcal{S}}_2$ contains the modified matrix $\mathcal{B}$ for which we want to apply the block Jacobi method. It is easy to see that the block diagonal matrix of $\hat{\mathcal{S}}_2$ is now positive definite whenever $\tau < 1$ which is for our time discretization scheme of course the case. Therefore, we propose to solve $\hat{\mathcal{S}}_2 y = g$ with a fixed number of steps of a block Jacobi method

$$y^{(l+1)} = y^{(l)} + \omega \mathcal{P}_2^{-1} r^{(l)},$$

where $\mathcal{P}_2$ contains the diagonal blocks of $\hat{\mathcal{S}}_2$. Of course, preconditioning the nonsmooth system is much more complicated than for the smooth one. Nevertheless, section 5 presents the performance of our preconditioner and shows quite good results.

5. Numerical Results

In this section we show results for the vector-valued Cahn–Hilliard problem. In each time step, we choose the sequence $\nu_1 = 10^{-1} \geq \nu_2 = 10^{-2} \geq \ldots \geq \nu_{\max} = 10^{-7}$ of penalty parameters and solve each corresponding subproblem $\mathbf{F}_{\nu_i}(\mathbf{u}_h^{(k)}, \mathbf{w}_h^{(k)})$ by the SSN method. In doing so, each Newton method is initialized by the approximate solution of the previous one. After the first time step we fix $\nu = \nu_{\max}$, i.e. from then on it suffices to solve only one SSN method per time step. This is because the initial solution at the beginning might not be a good starting point for the SSN methods. For the (smooth and nonsmooth) Newton method we use the stopping criterion in [24], given by

$$\|\mathbf{F}_\nu(\mathbf{u}_h^{(k)}, \mathbf{w}_h^{(k)})\|_2 \leq \epsilon_{\text{rel}}\,\|\mathbf{F}_\nu(\mathbf{u}_h^{(0)}, \mathbf{w}_h^{(0)})\|_2 + \epsilon_{\text{abs}}, \quad k = 1, \ldots, k_{\max},$$

where we set $k_{\max} = 20$, $\epsilon_{\text{rel}} = 10^{-12}$ and $\epsilon_{\text{abs}} = 10^{-6}$ in all examples. In each Newton step, we solve the linear system (17) by a Krylov subspace solver. The left preconditioners we have presented can be embedded into various of such iterative solvers. For our nonsymmetric system matrix $\mathcal{K}$ we propose the use of a nonsymmetric short-term recurrence method, namely BiCG. We set the BiCG tolerance to be 10^{-7} for the preconditioned relative residual in all examples. The FFT based preconditioner uses three steps of the inexact Uzawa method and the block Jacobi preconditioner uses five steps. For the multilevel approximations we choose Trilinos AMG approximations [22]. For one application of the preconditioner we take in general 10 steps of a Chebyshev smoother and two V-cycles. The discretization is performed with deal.II [1], which allows the use of the Trilinos library. All numerical experiments listed here are generated with finite elements on rectangles. Experiments show that it is essential to ensure that at least eight vertices lie on the interfaces to avoid mesh effects. Therefore, in all examples we set $\varepsilon \approx \frac{9h}{\pi}$. Concerning the time step, existence and uniqueness of corresponding discrete solutions of the nonsmooth system has been shown in [6, Theorem 2.4] under the condition $\tau < \frac{4\varepsilon^2}{\lambda_A^2 \|L\|}$, where λ_A is the largest positive eigenvalue of A and $\|L\|$ denotes the spectral norm of L. For the numerical examples presented here we choose $\tau \approx \frac{4\varepsilon^2}{(N-1)^2}$ if not mentioned otherwise. For the smooth system, we use the maximum time steps guaranteeing the stability of the time discretization scheme taken from [27]. These are in our computations $\tau \approx 4\varepsilon^2$. The domain is set to be $[0,1]^2$. For the initial condition, 100 circles with radius 0.0457–0.0525 are randomly distributed over Ω and randomly assigned to the different components.

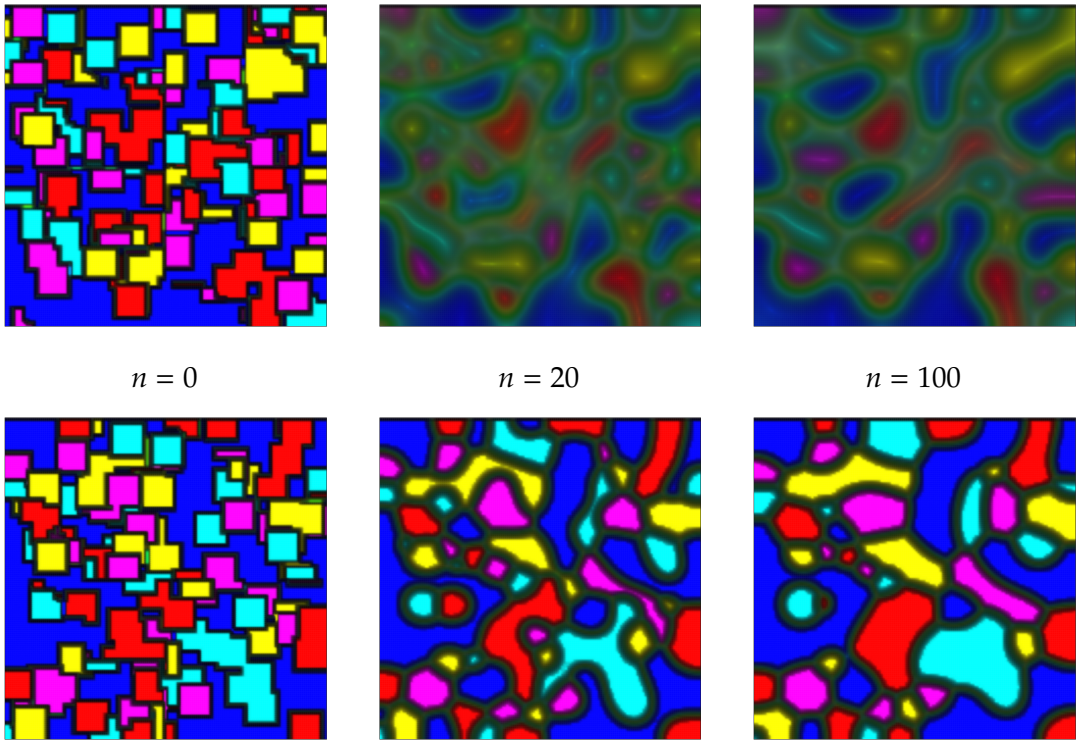

FIGURE 1. Smooth (above) and nonsmooth (below) computation for five phases.

In Figure 1, we compare the performance of the smooth and nonsmooth model. It shows the evolution of 5 phases over $n = 100$ time steps for a mesh with size $h = 2^{-8}$. For this example, we choose $\tau = 3 \cdot 10^{-4}$ in the nonsmooth model. Table 1 illustrates the minimum and maximum

value of the order parameter u_1. We see that the concentrations are closer to 0 and 1 in the nonsmooth model.

		time step				
		20	40	60	80	100
min	smooth	-0.02771	-0.02151	-0.02439	-0.02143	-0.02627
	nonsmooth	$-1.186 \cdot 10^{-7}$	$-1.174 \cdot 10^{-7}$	$-1.172 \cdot 10^{-7}$	$-1.204 \cdot 10^{-7}$	$-1.178 \cdot 10^{-7}$
max	smooth	0.9764	0.9803	1.001	0.9845	0.9972
	nonsmooth	1	1	1	1	1

TABLE 1. Minimum and maximum values of the order parameter u_1 in the smooth and nonsmooth model.

Next, we consider various uniform mesh sizes and compare the average number of BiCG iterations needed per Newton step over 50 time steps. Moreover, we test the robustness with respect to the number of phases. Figure 2 shows the results for the smooth model. In the legend of Figure 2(a) the number of degrees of freedom m and the average time needed for one Newton step is listed. The computations are done for $N = 7$ phases. The legend of Figure 2(b) shows the number of phases N and again the average time needed for one Newton step. Here, the computations are done for the mesh size $h = 2^{-8}$. In all calculations, the number of BiCG iterations does not exceed 16. The iteration numbers for the cases $L = I$ and $L = I - \frac{1}{N}\mathbf{1}\mathbf{1}^T$ are almost the same. Therefore, Figure 2 numerically shows the robustness of the preconditioner for both, the mesh size and the number of phases.

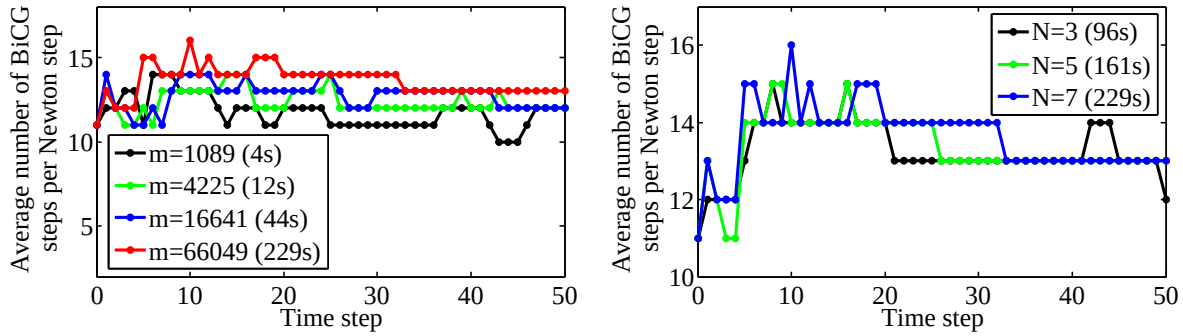

(A) $N = 7$. (B) $h = 2^{-8}$.

FIGURE 2. Results for 50 time steps of the smooth model.

The same computations are done with the nonsmooth model, where we use in Figure 3a five phases and in Figure 3b the mesh size $h = 2^{-7}$. Additionally, we compare the average BiCG iteration numbers with and without preconditioning for the first time step in Figure 4. Here, the number of phases is three. As mentioned in the beginning of this section, we solve within this first time step 7 Newton methods for the penalty parameters $\nu_1 = 10^{-1}, \dots, \nu_7 = 10^{-7}$, respectively. As can be seen from this, although the preconditioned iteration numbers are considerably worse compared to the one in the smooth model, the preconditioned version always outperforms the unpreconditioned method. A factor of 1500 (3500) for $h = 2^{-5}$ ($h = 2^{-6}$) can be observed and we would expect this to be even more significant if a larger number of phases or degrees of freedom is used.

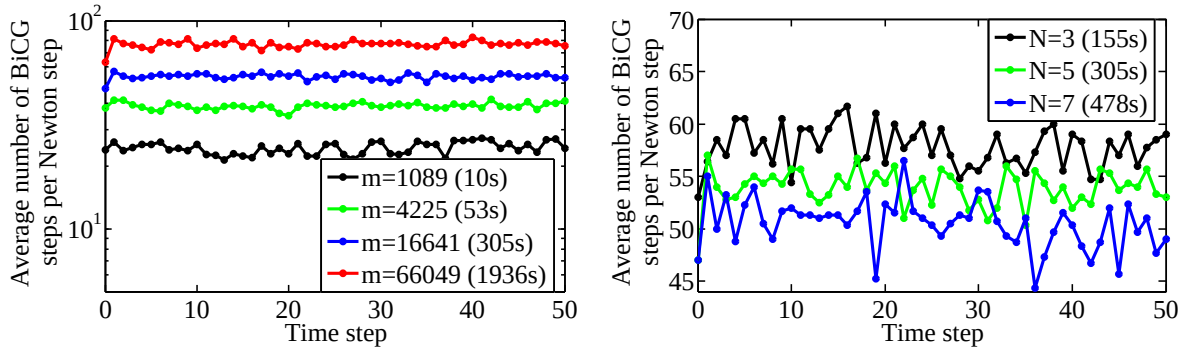

(A) $N = 5$. (B) $h = 2^{-7}$.

FIGURE 3. Results for 50 time steps of the nonsmooth model.

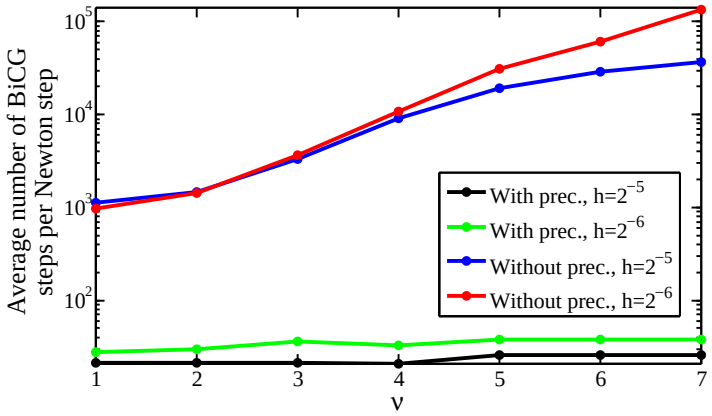

FIGURE 4. Preconditioning vs. no preconditioning in the nonsmooth model.

6. Conclusions

In this paper we have analyzed the linear systems arising in smooth and nonsmooth vector-valued Cahn–Hilliard systems. For the latter, we have applied an SSN method combined with a Moreau-Yosida regularization technique for handling the pointwise constraints. In order to make the SSN method more efficient we have used a Krylov subspace solver. We have introduced and studied block-triangular preconditioners using an efficient Schur complement approximation. This approximation can be done using multilevel techniques, such as AMG (as in our case), and the numerical results justify this choice.

Acknowledgements

The author would like to thank Martin Stoll, Luise Blank and Harald Garcke for their helpful comments and suggestions.

References

[1] W. Bangerth, R. Hartmann, and G. Kanschat, *deal.II — a general purpose object oriented finite element library*, ACM Trans. Math. Software, 33 (2007), pp. 24/1–24/27.

[2] J.W. Barrett and J.F. Blowey, *An error bound for the finite element approximation of a model for phase separation of a multi-component alloy*, IMA J. Numer. Anal., 16 (1996), pp. 257–287.

[3] ———, *Finite element approximation of a model for phase separation of a multi-component alloy with non-smooth free energy*, Numer. Math., 77 (1997), pp. 1–34.

[4] L. Blank, H. Garcke, L. Sarbu, and V. Styles, *Primal-dual active set methods for Allen-Cahn variational inequalities with nonlocal constraints*, Numer. Methods Partial Differ. Equ., (2012).
[5] ———, *Nonlocal Allen-Cahn systems. Analysis and a primal-dual active set method.*, IMA J. Numer. Anal., 33 (2013), pp. 1126–1155.
[6] J.F. Blowey, M.I.M. Copetti, and C.M. Elliott, *Numerical analysis of a model for phase separation of a multi-component alloy.*, IMA J. Numer. Anal., 16 (1996), pp. 111–139.
[7] J. Bosch, D. Kay, M. Stoll, and A.J. Wathen, *Fast Solvers for Cahn-Hilliard Inpainting*, SIAM J. Imaging Sci., to appear, (2013).
[8] J. Bosch, M. Stoll, and P. Benner, *Fast solution of Cahn-Hilliard variational inequalities using implicit time discretization and finite elements*, J. Comput. Phys., to appear, (2013).
[9] M. Butz, *Computational methods for Cahn-Hilliard variational inequalities*, PhD thesis, University of Regensburg, Regensburg, Germany, 2012.
[10] J.W. Cahn and J.E. Hilliard, *Free energy of a nonuniform system. I. Interfacial free energy*, J. Chem. Phys., 28 (1958), pp. 258–267.
[11] M. Chen, *On the solution of circulant linear systems*, SIAM J. Numer. Anal, 24 (1987), pp. 668–683.
[12] T.A. Davis, *UMFPACK Version 4.4 User Guide*, tech. report, Department of Computer and Information Science and Engineering, University of Florida, Gainesville, FL, 2005.
[13] I.C. Dolcetta, S.F. Vita, and R. March, *Area-preserving curve-shortening flows: From phase separation to image processing*, Interfaces Free Bound., 4 (2002), pp. 325–343.
[14] C.M. Elliott and H. Garcke, *Diffusional phase transitions in multicomponent systems with a concentration dependent mobility matrix*, Phys. D, 109 (1997), pp. 242–256.
[15] C.M. Elliott and S. Luckhaus, *A generalised diffusion equation for phase separation of a multi-component mixture with interfacial free energy*, Preprint 195, University of Bonn, Bonn, Germany, 1991.
[16] H.C. Elman, D.J. Silvester, and A.J. Wathen, *Finite Elements and Fast Iterative Solvers: With Applications in Incompressible Fluid Dynamics*, Oxford University Press, Oxford, UK, 2005.
[17] D.J. Eyre, *Systems of Cahn-Hilliard equations*, SIAM J. Appl. Math., 53 (1993), pp. 1686–1712.
[18] H. Garcke, *Mechanical effects in the Cahn-Hilliard model: A review on mathematical results*, in Mathematical Methods and Models in Phase Transitions, A. Miranville, ed., Nova Science, New York, 2005, pp. 43–77.
[19] H. Garcke, B. Nestler, and B. Stoth, *On anisotropic order parameter models for multi-phase systems and their sharp interface limits*, Phys. D, 115 (1998), pp. 87–108.
[20] ———, *A multi phase field concept: Numerical simulations of moving phasee boundaries and multiple junctions*, SIAM J. Appl. Math., 60 (1999), pp. 295–315.
[21] A. Greenbaum, *Iterative Methods for Solving Linear Systems*, vol. 17 of Frontiers Appl. Math., SIAM, Philadelphia, 1997.
[22] M.A. Heroux, R.A. Bartlett, V.E. Howle, R.J. Hoekstra, J.J. Hu, T.G. Kolda, R.B. Lehoucq, K.R. Long, R.P. Pawlowski, E.T. Phipps, A.G. Salinger, H.K. Thornquist, R.S. Tuminaro, J.M. Willenbring, A. Williams, and K.S. Stanley, *An Overview of Trilinos*, Tech. Report SAND2003-2927, Sandia National Laboratories, Albuquerque, NM, 2003.
[23] J.E. Hilliard and J.W. Cahn, *An evaluation of procedures in quantitative metallography for volume-fraction analysis*, Trans. Am. Inst. Min. Metall. Eng., 221 (1961), pp. 344–352.
[24] M. Hintermüller, M. Hinze, and M.H. Tber, *An adaptive finite-element Moreau-Yosida-based solver for a non-smooth Cahn-Hilliard problem*, Optim. Methods Softw., 26 (2011), pp. 777–811.
[25] M. Hintermüller, K. Ito, and K. Kunisch, *The primal-dual active set strategy as a semismooth Newton method*, SIAM J. Optim., 13 (2003), pp. 865–888.
[26] D. Kay and A. Tomasi, *Colour image segmentation by the vector-valued Allen-Cahn phase-field model: a multigrid solution*, IEEE Trans. Image Proc., 18 (2007).
[27] H.G. Lee, J.-W. Choi, and J. Kim, *A practically unconditionally gradient stable scheme for the N-component Cahn-Hilliard system*, Phys. A, 391 (2012), pp. 1009 – 1019.
[28] J.E. Morral and J.W. Cahn, *Spinodal decomposition in ternary systems*, Acta Metall., 19 (1971), pp. 1037 – 1045.
[29] M.F. Murphy, G.H. Golub, and A.J. Wathen, *A note on preconditioning for indefinite linear systems*, SIAM J. Sci. Comput., 21 (2000), pp. 1969–1972.
[30] J.W. Ruge and K. Stüben, *Algebraic multigrid*, in Multigrid methods, vol. 3 of Frontiers Appl. Math., SIAM, Philadelphia, 1987, pp. 73–130.
[31] I. Steinbach, F. Pezzolla, B. Nestler, M. Seeßelberg, R. Prieler, G.J. Schmitz, and J.L.L. Rezende, *A phase field concept for multiphase systems*, Phys. D, 94 (1996), pp. 135–147.
[32] M. Stoll, *One-shot solution of a time-dependent time-periodic PDE-constrained optimization problem*, IMA J. Numer. Anal., to appear, (2013).
[33] X.-F. Wu and Y.A. Dzenis, *Phase-field modeling of the formation of lamellar nanostructures in diblock copolymer thin films under inplanar electric fields*, Phys. Rev. E, 77 (2008), pp. 031807/1–031807/10.